Jour. of the KGS, Vol. 23, No. 3. March 2007, pp. 101~109

Effect of Fines on the Stability of Unsaturated Soil Slopes

불포화 사면안정에 미치는 세립분의 영향분석

Lee, Kyu-Hyun[1] 이 규 현
Jeong, Sang-Seom[2] 정 상 섬
Kim, Tae-Hyung[3] 김 태 형

요 지

국내 풍화토사면의 경우 순수 균질 사면보다는 대부분 점토 및 세립분이 섞인 비균질 상태로 존재하며 이러한 함유비율은 풍화도 및 지역에 따라 다르다. 따라서 세립분함량 변화에 따른 불포화사면에의 분석을 위해, 화강풍화토(SW)에 일정비율의 세립분(CH)을 섞어 성형한 시료를 통해 GCTS pressure plates을 이용한 함수특성곡선 실험을 수행하였다. 실험 및 침투해석결과 강우지속시간에 따른 포화깊이의 증가율은 세립분이 증가할수록 또한 상대밀도가 증가할수록 작아졌다. 또한 침투해석과 포화 및 불포화강도정수를 이용한 사면 안정성 해석결과(SLOPE/W), 전반적으로 세립분함량 10~15%의 범위까지는 침투깊이 증가에 따른 흡수력 변화가 안전율에 지대한 영향을 미치는 반면 이를 초과하는 경우(>15%)에는 오히려 세립분함량 증가에 따른 강도정수의 변화가 크게 영향을 미침을 알 수 있었다.

Abstract

In South Korea, many weathered soil slopes are composed of soil mixtures with certain amount of clay fractions in natural soil deposits. Accordingly, it is very important to analyze that effect of the fines on the stability of unsaturated soil slopes. In this study, five different soil types classified by mixture portion of fines were used and experiment on the soil-water characteristic curve tests (SWCC) using GCTS (Geotechnical Consulting and Testing Systems) pressure plate were performed in order to analyze the stability of unsaturated soil slopes. Based on the infiltration analysis which contains SWCC test result by the SEEP/W, it is shown that the increasing rate of the wetting band depth was decreased as the fines content and the relative density were increased. According to the stability analysis result of the unsaturated soil slopes through the SLOPE/W, it is found that the transition from the wetting band depth to the variation of strength parameters which affect the stability of unsaturated soil slopes appears to occur around 10~15% of clay contents in the mixtures.

Keywords : GCTS pressure plate, Infiltration analysis, Strength parameters, SWCC, Wetting band depth

1. Introduction

Effective factors of rock slopes stability due to rainfall are the value of water pressure in vertical joint or in tension-cracks and up-lift water pressures on sliding plane (s). On the other hand, in case of the stability analysis on unsaturated soil slopes, the wetting band depth due to rainfall is the main reason of unsaturated soil slope

1 Researcher, Civil Research & Eng. Team, Technology Research Institute, Daelim Industrial Co., Ltd.
2 Member, Prof., Dept. of Civil Eng., Yonsei Univ., soj9081@yonsei.ac.kr
3 Graduate Student, Dept. of Civil Eng., Yonsei Univ., tvnimph@hotmail.com

failure. Accordingly, it is very important to analyze the wetting band depth due to rainfall for unsaturated soil slopes.

Most of the land area of Korean peninsula are composed of soils formed from the in situ weathering of granite and genesis. Many slope failures in these weathered failure of these weathered soils are triggered by heavy rainfall. These failures are characterized by relatively shallow failure surfaces that develop parallel to the original slope. These failures may be attributed to the deepening of a wetting front into the slope due to rainfall infiltration which results in an increase in moisture content, a decrease in soil matric suction and a decrease in shear strength on the potential failure surface (Ng and Shi, 1998; Fourie et al., 1999; Lee et al., 2002; Kim et al., 2004). It is generally said that the unsaturated soil slope failures due to rainfall are mainly caused by the decrease in suction of unsaturated soil with the increase of the water content and wetting band depth.

In South Korea, many weathered soils can be classified as SW or SM according to the Unified Soil Classification System (USCS). These soils consist of soil mixture with certain amount of clay fractions in natural soil deposits. This paper describes the results of a series of soil-water characteristic curve tests and numerical analyses aimed at clarifying the effect of the magnitude of wetting band depth on unsaturated soil slopes. Special attention is given to the prediction of approximate limit of clay content which influences the magnitude of wetting band depth in soil mixtures.

2. Soil-Water Characteristic Curve Testing

The soil suction, generally called 'total suction', consists of matric and osmotic suctions. Soil suction is commonly referred to as the free energy state of soil water. For groundwater flow through an unsaturated soil, the coefficient of permeability is not a constant but a function of soil suction. Therefore, it is necessary to determine the soil-water characteristic curve (SWCC) that defines the relationship between the suction and the volumetric water content of the soil. This curve can be used to derive permeability functions for use in unsaturated groundwater flow problems (Fredlund and Rahardjo, 1993). It is also possible to use SWCC to establish unsaturated shear strength parameters (Vanapalli et al., 1996).

2.1 Description of the Apparatus

The GCTS pressure plate was developed by Fredlund in 2005. The GCTS pressure plate uses the axis-translation

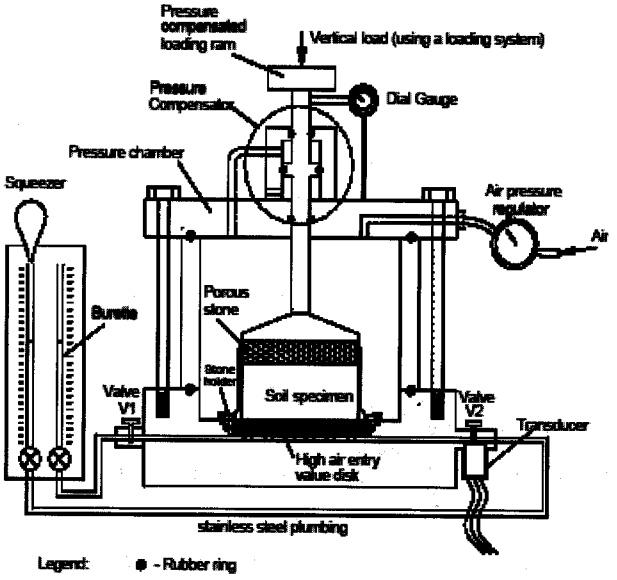

(a) Schematic of the GCTS pressure plate

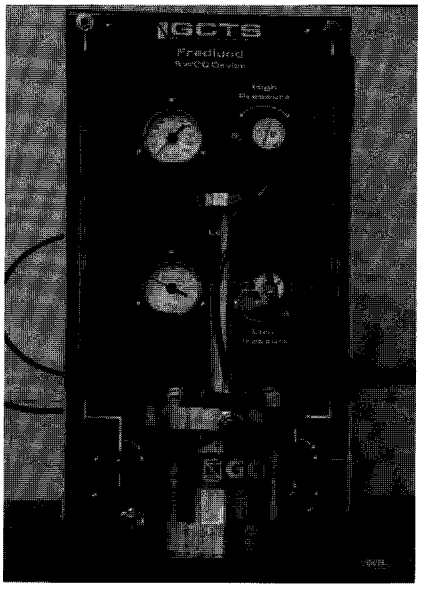

(b) Photo of the GCTS pressure plate measuring for SWCC

Fig. 1. The GCTS pressure plate

technique to control matric suction in the soil specimen (Fredlund and Rahardjo, 1993). The GCTS pressure plate consists of two main parts (Fig. 1) which are a pressure chamber and a loading system. The pressure chamber was designed for measuring soil-water characteristic curves. The pressure chamber is stainless steel and can be subjected to extremely high air pressure. The soil specimen is rammed into a stainless steel ring and placed on top of the high air entry ceramic stone. Different high air entry ceramic stones can be inserted into the base of the apparatus and used for different soil types. It is also possible to use a range of ceramic stone on one soil that is tested over a wide range of matric suction (i.e., 1 bar, 3 bars, 5 bars and 15 bars). The apparatus is capable of testing the soil specimen over a wide range of matric suction from 1 kPa to 1000 kPa. At a low soil suction (i.e., from 1 kPa to 10 kPa), a hanging burette can be attached to provide an accurate value of soil suction to the soil specimen. At higher soil suctions (i.e., from 3 kPa to 1000 kPa) the axis-translation technique is used. Dual pressure gauge (i.e., a high pressure gauge and a low pressure gauge) and regulators are designed to accurately control the applied soil suction over the entire range.

The bottom of the pressure chamber (i.e., below the ceramic stone) is connected to two burettes. The amount of water drained out (i.e., drying process) or absorbed into the soil specimen (i.e., wetting process) can be measured using the two burettes. The burettes can be connected to a squeezer that is used to flush diffused air from the bottom of the pressure chamber.

2.2 Materials

The soils used in this study are weathered soil (SW) and clay soil (CH) in Korea. The grain-size distribution curves of weathered soil (SW) are shown in Fig. 2 and the plasticity chart of clay soil (CH) is shown in Fig. 3. The weathered soil had a liquid limit, LL = 28.7, plastic limit, PL = 21.35, specific gravity, G_s = 2.683. The clay soil had a liquid limit, LL = 63, plastic limit, PL = 29.3, specific gravity, G_s = 2.604.

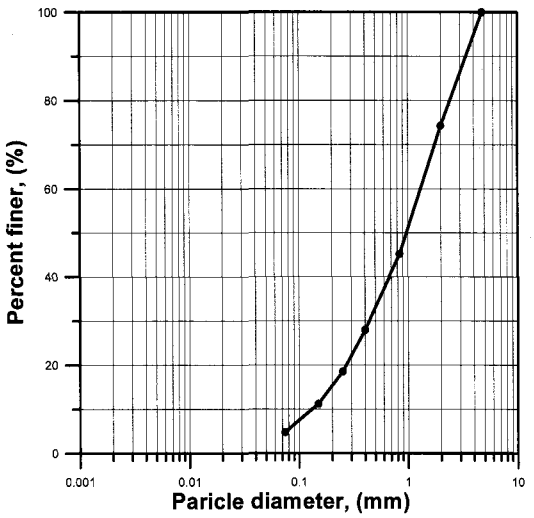

Fig. 2. Grain-size distribution curves (SW)

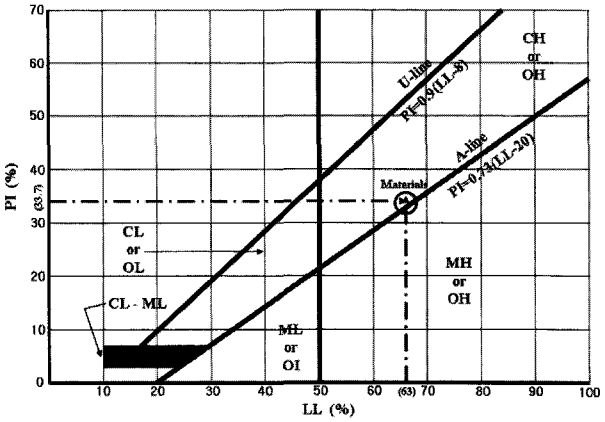

Fig. 3. Plasticity chart (CH)

For measuring soil-water characteristic curves, sample with different clay contents of 0%, 5%, 10%, 15%, and 20% were formed. The soil-water characteristic curve and coefficient of permeability were measured for different densities (D_r = 70, 90%). In case of the 70% densities, all of the clay contents were used and in case of the 90% densities, 3 clay contents (i.e., 10%, 15%, 20%) were used.

2.3 Testing Procedures

A solid stainless steel with diameter of 60 mm and a height of 30 mm was substituted for soil specimen. It was assumed that the solid stainless steel was rigid and did not deform (i.e., a K_0 condition). The amount of water in the burettes was recorded under various soil suctions.

In order to measure the soil-water characteristic curve

of the soil specimens in the GCTS pressure plate, specimens were compacted by the ramming. The following procedures were used to prepare a soil specimen : (1) Calculate the γ_{min} and γ_{max}, (2) Decide the weight of soil by the relative densities of 70% and 90%, (3) Compact the soil mixtures in the solid stainless steel by the ramming (Fig. 4), (4) Submerge (saturate) the soil specimen (Fig. 5).

The saturated soil specimen is placed on a saturated ceramic disk and mounted on the bottom plate. The ceramic disk acts like a semi-permeable medium and allows water, but not air, to pass through the disk up to a rated air pressure value (i.e., air-entry value of the ceramic). The bottom of the ceramic disk is maintained more or less at atmospheric pressure by connecting the drain holes to two tubes filled with water. The applied air pressure represents the applied matric suction. In response to the applied suction the water moves out of the soil specimen and drains through the ceramic disk until the equilibrium is established. The magnitude of the applied matric suction is the same for each soil specimen (i.e., 4, 10, 20, 40, 100, 200 and 400 kPa).

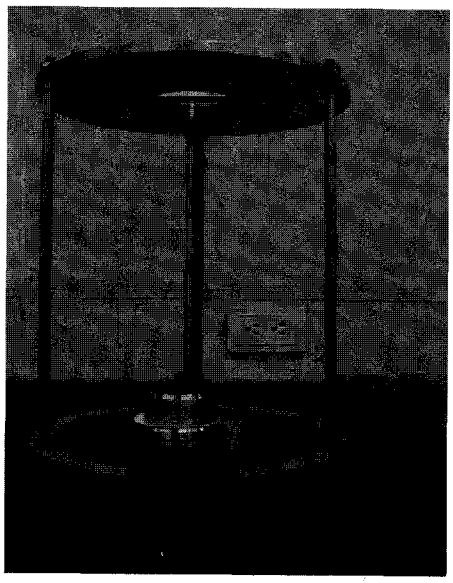

Fig. 4. Compaction of the soil mixtures

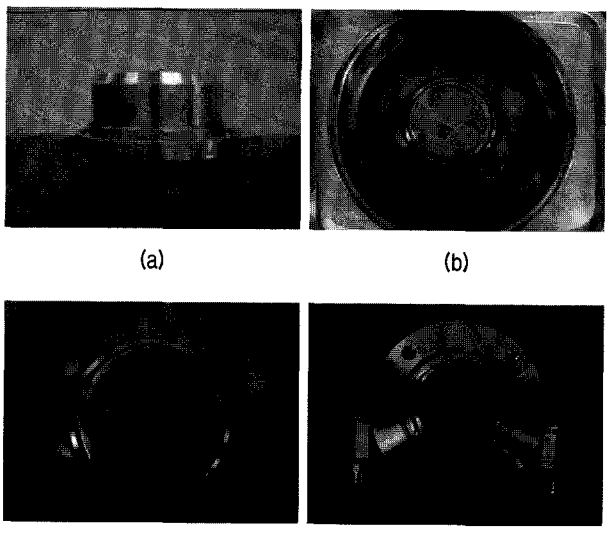

(a) (b)

(c) (d)

Fig. 5. Preparation of the soil specimen

2.4 Discussion on the Test Results for Soil-Water Characteristic Curve

The GCTS pressure plate was used for defining the SWCC for each soil mixtures. The values of a, m and n used in the Fredlund & Xing's SWCC equation (1994) (Eq. 1) are given in Table 1.

$$\theta = C(\psi)\frac{\theta_s}{\ln[e+(\psi/a)^n]^m} \quad (1)$$

where $C(\psi)$ is the correction function, θ is the volumetric water content, θ_s is the saturated volumetric water content, e is the natural number (2.71828), ψ is the negative pore-water pressure (suction), and a, n and m are curve fitting parameters

The results of the soil-water characteristic curve tests are shown Fig. 6. It is difficult to compare the results of the SWCC tests for each soil mixtures, because the saturated volumetric water content at saturation is different according to each soil mixture to compare the results of the SWCC test for each soil mixtures, the volumetric water content was normalized by the initial volumetric water content. As you see the Fig. 6, the volumetric water content decrement was decreased as the fines content of each soil mixture was increased. And the volumetric water content had critical differences between SW100% and other soil mixture (SW95%+CH5%, SW90%+CH10%, SW85%+CH15%, SW80%+CH20%). However, there were no notable distinctions on soils that were mixed with some fines.

Table 1. Curve-fitting parameters for the SWCC

	D_r=70%					D_r=90%		
	SW100	SW95	SW90	SW85	SW80	SW90	SW85	SW80
a	4.811	8.819	5.452	7.827	8.368	9.283	8.164	9.477
n	2.536	8.637	1.690	1.305	1.849	2.515	2.366	1.51
m	0.637	0.151	0.27	0.302	0.221	0.294	0.226	0.217

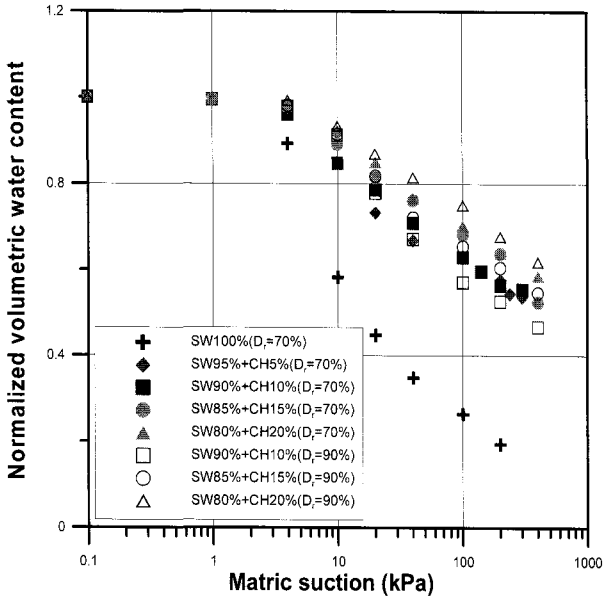

Fig. 6. Test results of the SWCC

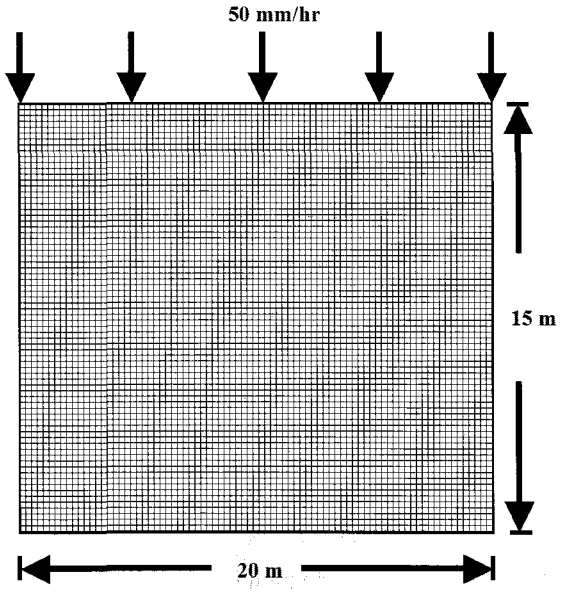

Fig. 7. Finite element mesh (seepage analysis)

3. Transient Finite Element Seepage and Theoretical Analysis

Transient seepage analyses of rainfall infiltration were carried out by means of the two-dimensional finite element program SEEP/W (Geo-Slope, 2004). The finite element mesh used in these analyses is shown in Fig. 7. The groundwater table is located at the bedrock-weathered soil interface. The top boundary is subjected to a rainfall intensity that is equal to the saturated permeability of the weathered soil to ensure downward infiltration into the weathered soil layer. Actually measuring the hydraulic conductivity function is a time-consuming and expansive procedure, but the function which was used by SEEP/W can be readily developed using measured volumetric water content function (i.e., SWCC) and the saturated hydraulic conductivity (Table 2). The results of hydraulic conductivity which were used in seepage analysis are shown in Fig. 8.

The total duration of rainfall is 96 hours. It was divided into 11 time stages (0.1, 0.5, 1, 2, 3, 5, 10, 24, 48, 72 and 96 hours) and wetting band depth was obtained for each of these stages. For simplicity, the intensity of rainfall was kept constant for the entire duration of rainfall. Similarly, the wetting band depth from a transient seepage analysis is calculated as the normal distance from the surface of the mesh at which a contour of -0.2 m pressure head is located. The contour for -0.2 m pressure head is chosen based on the observation from slope stability analysis that normal distance between the critical

Table 2. Coefficient of permeability at saturation (m/s)

	D_r=70%					D_r=90%		
	SW100	SW95	SW90	SW85	SW80	SW90	SW85	SW80
K_{sat} (m/s)	5.05×E−6	1.13×E−6	7.84×E−7	5.87×E−7	2.58×E−7	2.94×E−7	7.84×E−8	3.45×E−8

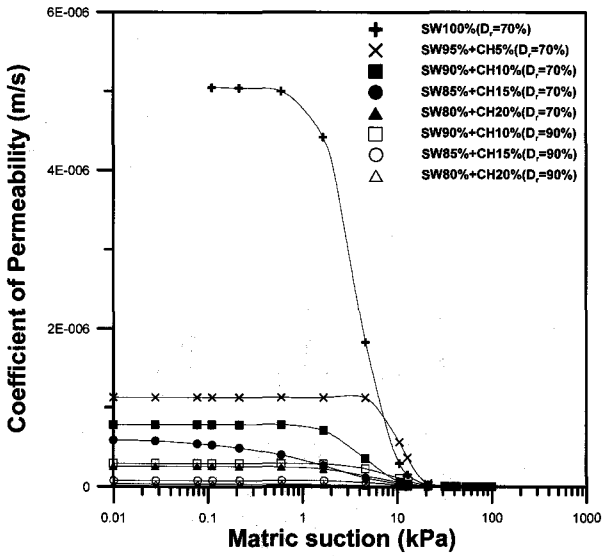

Fig. 8. K vs. matric suction

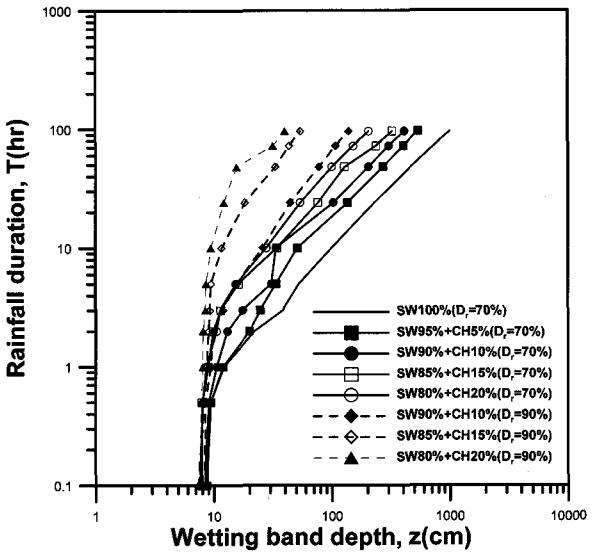

Fig. 9. Wetting band depth vs. rainfall duration

failure plane and the surface of the slope was always equal to normal distance between this contour and the surface of the slope (Kim et al., 2006).

It is shown that increase of the fines content affects the decrease of the infiltration rate for all soil mixtures (Fig. 9). And the increasing rate of wetting band depth was decreased as the fines contents in the mixtures and the relative densities were increased. Theses results come from the decrease of coefficient of permeability and the increase of the soil suction (Fig. 8).

4. An Internal Friction Angle Associated with Matric Suction(ϕ^b)

Generally, an internal friction angle associated with matric suction which is called the ϕ^b is obtained by the unsaturated soil triaxial test. However, establishing the triaxial test on unsaturated soils needs lots of time and has some difficulties in operation. For an alternative solution, it has been investigated in different ways in order to define ϕ^b. Fortunately, Vanapalli et al. (1996) already defined the relationship between internal friction angle and internal friction angle of unsaturated soils (i.e., ϕ^b). For the friction angle of unsaturated soils, Eq. 2 (Vanapalli et al., 1996) in this study is used.

$$\tan(\phi^b) = \tan(\phi')\left(\frac{\theta-\theta_r}{\theta_s-\theta_r}\right) \quad (2)$$

where ϕ' is the angle of internal friction, θ is the volumetric water content, θ_r is the residual volumetric water content (Table 3), θ_s is the saturated volumetric water content and ϕ^b is the angle indicating the rate of increase in shear strength to the matric suction.

Because the volumetric water content was decreased as the matric suction was increased, the internal frictional angle associated with matric suction was decreased as the matric suction was increased (Fig. 10).

5. Numerical Analysis of the Stability of Unsaturated Soil Slopes

In order to evaluate the effect of wetting band depth and magnitude of the matric suction on the stability of

Table 3. The residual volumetric water content

	D_r=70%					D_r=90%		
	SW100	SW95	SW90	SW85	SW80	SW90	SW85	SW80
θ_r	0.038	0.034	0.017	0.026	0.035	0.017	0.026	0.035

Note : θ_r is the value observed by the filter paper method (Yu, 2003)

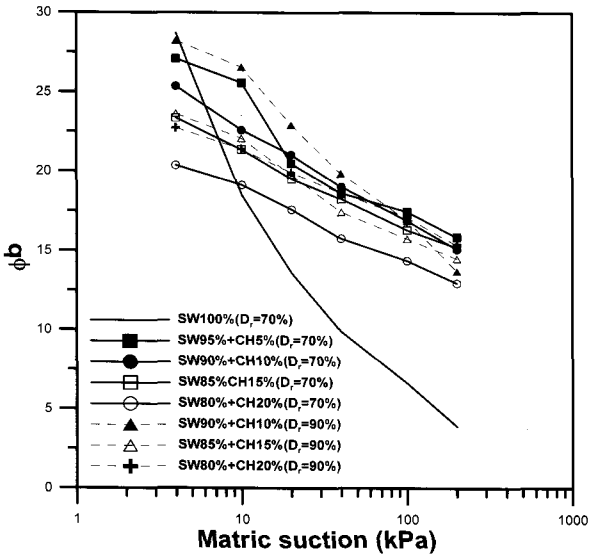

Fig. 10. ϕ^b vs. matric suction

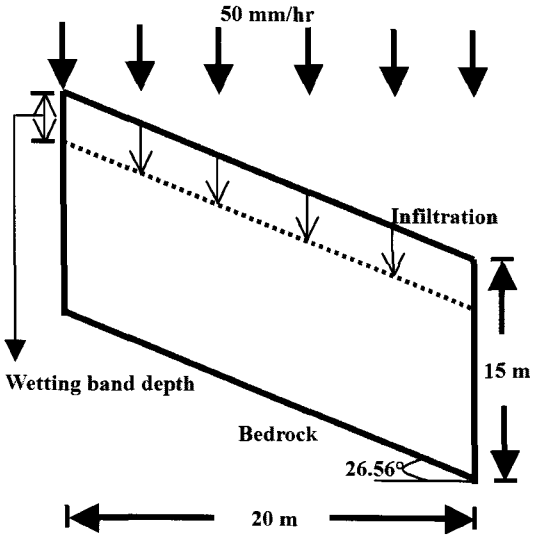

Fig. 11. Finite element mesh (SLOPE/W)

slopes in unsaturated soils, three sets of analysis were conducted using the limit equilibrium based on SLOPE/W program (GEO-SLOPE, 2004). Three infinite slopes – inclined at 26°, 33°, 45° – were considered, and strength parameter, such as ϕ', ϕ^b and c' of each mixed soil was fixed as properties of each mixed soil to identify the relation to the only wetting band depth due to rainfall in a slope (Fig. 11). The stability of unsaturated soil slope is analyzed with assumption that the bottom part of infinite slope would be bedrock and the finite element mesh(SLOPE/W) used in this study is shown in Figure 11.

The physical properties of soil mixtures are shown in Table 4. It is shown that the internal frictional angle was decreased as the fines content was increased. But the internal frictional angle was increased as the relative density was increased.

Figure 12 and Figure 13 show the analyzing results of the unsaturated soil slope stability. X-axis means the amount of matric suction with varying volumetric water content when measuring SWCC. If the factor of safety was only affected by the magnitude of wetting band depth, it must increase as the fines content was increased in soil mixtures. However, the factor of the safety decreased by a certain point – slope containing 20% fines content inclined to 26° and 33° hardened 70% relative density came to have 15% fines content inclined to 45° and hardened 70% relative density (Fig. 12), and any slope contained 15% fines content and hardened 90% relative density (Fig. 13). This means that the effect of the wetting band depth on slope stability is somewhat limited to fine content in soil mixtures. That is, the factor of safety is affected by the wetting band depth rather than the variation of strength parameters as the fines content increase, especially the fines content increases as much as 10~15% approximately.

Table 4. Physical properties of soil mixtures

Soil Mixtures	γ_d (kN/m^3)	γ_{sat} (kN/m^3)	c' (kN/m^2)	ϕ' (°)
SW100% (D_r=70%)	11.976	15.889	0	31.84
SW95% (D_r=70%)	12.877	16.482	12.847	27.75
SW90% (D_r=70%)	13.22	16.836	22.948	26.32
SW85% (D_r=70%)	13.436	17.444	26.086	23.85
SW80% (D_r=70%)	13.524	17.655	28.635	20.75
SW90% (D_r=90%)	13.507	17.367	14.21	28.78
SW85% (D_r=90%)	13.782	17.867	16.856	24.03
SW80% (D_r=90%)	14.148	18.202	25.284	22.89

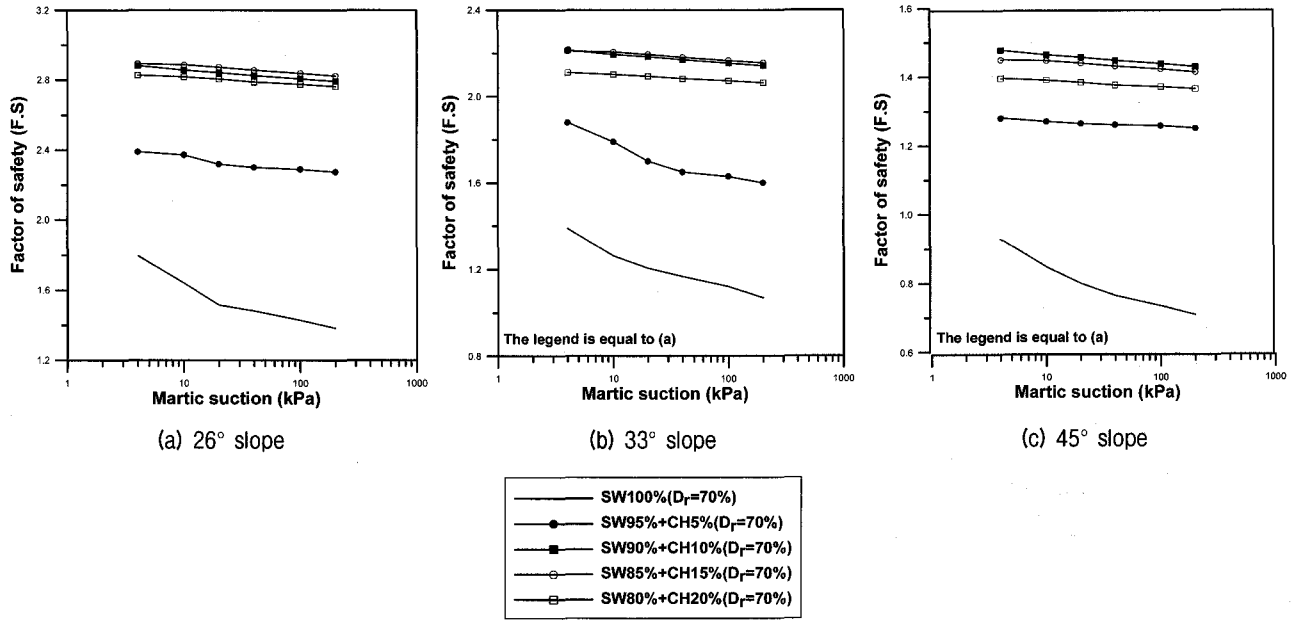

Fig. 12. Factor of safety concerning soil mixtures (D_r=70%)

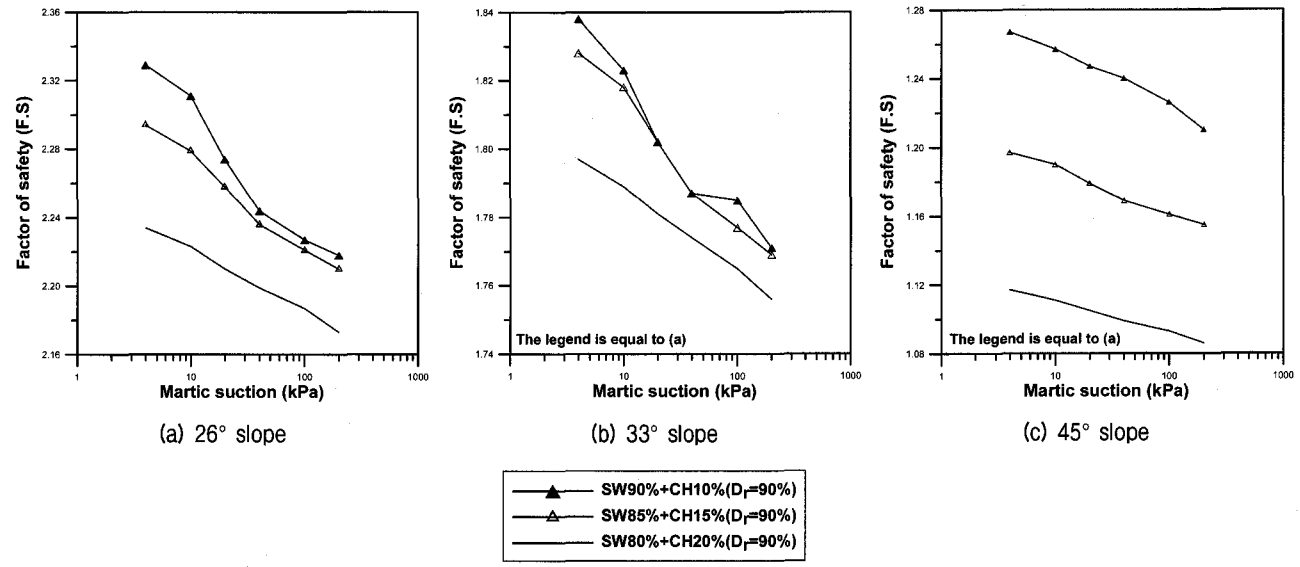

Fig. 13. Factor of safety concerning soil mixtures (D_r=90%)

Besides this range, it is affected by the variation of the strength parameters as the fines content increases.

6. Conclusion

(1) The volumetric water content decrement was decreased as the fines content of the each soil mixtures and the relative densities were increased. And the volumetric water content had critical distinction between SW100% and other soil mixtures (SW95%+CH5%, SW90%+CH10%, SW85%+CH15%, SW80%+CH20%).

(2) The increasing rate of the wetting band depth was decreased as the fines contents in the mixtures and the relative densities were increased. These results come from the decrease of the coefficient of permeability and the increase of the soil suction.

(3) According to the stability analysis result of the unsaturated soil slopes through the SLOPE/W, it is found that the transition from the wetting band depth to the variation of strength parameters which affect the stability of unsaturated soil slopes appears to occur around 10~15% of clay contents in the mixtures.

References

1. Collins, B.D., Znidarcic, D.Z. (2004), "Stability analyses of rainfall induced landslides", *Journal of Geotechnical and Environmental Eng.*, Vol.130, No.4, pp.362-372.
2. Fourie, A.B., Rowe, D. and Blight, G.E. (1999), "The effect of infiltration on the stability of the slope of a dry ash dump", *Geotechnique*, Vol.49, No.1, pp.1-13.
3. Fredlund, D.G. and Rahardjo, H. (1993), *Soil mechanics for unsaturated soils*, John Wiley and Sons, New York, pp.217-259.
4. Fredlund, D.G., Xing, A. and Huang, A. (1994), "Predicting the permeability function for unsaturated soils using the soil-water characteristic curve", *Canadian Geotechnical Journal*, Vol.31, pp.533-546.
5. Fredlund, D.G. and Xing, A. (1994), "Equation for the soil-water characteristic curve", *Canadian Geotechnical Journal*, Vol.31, pp.521-532.
6. Geo-slope. (2004), *User manual for SEEP/W and SLOPE/W. version 6*, Canada, Geo-Slope International Ltd.
7. Kim, J. (2002), *Stability analysis on unsaturated weathered infinite slopes based on rainfall-induced wetting*, Master of Eng. Thesis, Yonsei University.
8. Kim, J., Jeong, S., Park, S. and Sharma. J. (2004), "Influence of rainfall-induced wetting on the stability of slopes in weathered soils", *Engineering Geology*, Vol.75, pp.251-262.
9. Kim, J., Park, S. and Jeong, S. (2006), "Effect of wetting front suction loss on stability of unsaturated soil slopes", *Proceedings of Sessions of Geoshanghai*, Geotechnical special publication No. 148, pp.70-77.
10. Lee, S.J., Lee, S.R. and Jang, B. (2002), "Unsaturated shear strength characteristics of weathered granite soils", *The Journal of Korean Society of Civil Engineers*, Vol.22, No.1, pp.81-88.
11. Lu, N., Likos, W. (2004), *Unsaturated soil mechanics*, John Wiley and Sons, New York, pp.220-241.
12. Ng, C.W.W., Shi, Q. (1998), "A numerical investigation of the stability of unsaturated soil slopes subjected to transient seepage", *Computer and Geotechnics*, Vol.22, No.1, pp.1-28.
13. Ng, C.W.W., Zhan, L.T., Bao, C.G., Fredlund, D.G. amd Gong, B.W. (2003), "Performance of an unsaturated expansive soil slope subjected to artificial rainfall infiltration", *Geotechnique*, Vol.53, No.2, pp.143-157.
14. Padilla, J.M., Perera, Y.Y., Houston, W.N. and Fredlund, D.G., "A new soil-water characteristic curve device".
15. Pham, H.Q., Fredlund, D.G. and Padilla, J.M., "Use of the GCTS apparatus for the measurement of soil- water characteristic curves".
16. Vanapalli, S.K., Fredlund, D.G., Pufahl, D.E. and Clifton, A.W. (1996), "Model for the prediction of shear strength with respect to soil suction", *Canadian Geotechnical Journal*, Vol.33, pp.379-392.
17. Yu, N. (2003), *Characteristics of unsaturated weathered soils with varying clay contents*, Master of Eng. Thesis, Yonsei University.

(received on Jan. 17, 2007, accepted on Mar. 20, 2007)